HHS Public Access

Author manuscript

Biomaterials. Author manuscript; available in PMC 2017 November 01.

Published in final edited form as:

Biomaterials. 2016 November ; 108: 168–176. doi:10.1016/j.biomaterials.2016.09.004.

Immunomodulatory nanoparticles ameliorate disease in the *Leishmania (Viannia) panamensis* mouse model

Alyssa L. Siefert[1,5], **Allison Ehrlich**[2,5], **María Jesús Corral**[3], **Karen Goldsmith-Pestana**[2], **Diane McMahon-Pratt**[2], and **Tarek M. Fahmy**[1,4]

[1]Yale School of Engineering and Applied Science, Department of Immunobiology, New Haven, CT USA

[2]Yale School of Public Health, Department of Immunobiology, New Haven, CT USA

[3]Department of Animal Health, Faculty of Veterinary Medicine, Universidad Complutense de Madrid, Madrid, Spain

[4]Yale Medical School, Department of Immunobiology, New Haven, CT USA

Abstract

Leishmania (Viannia) panamensis (*L. (V.) panamensis*) is a species of protozoan parasites that causes New World leishmaniasis, which is characterized by a hyper-inflammatory response. Current treatment strategies, mainly chemotherapeutic, are suboptimal due to adverse effects, long treatment regimens, and increasing drug resistance. Recently, immunotherapeutic approaches have shown promise in preclinical studies of leishmaniasis. As NPs may enable broad cellular immunomodulation through internalization in phagocytic and antigen-presenting cells, we tested the therapeutic efficacy of biodegradable NPs encapsulating a pathogen-associated molecular pattern (PAMP), CpG-rich oligonucleotide (CpG; NP-CpG), in mice infected with *L. (V.) panamensis*. NP-CpG treatment reduced lesion size and parasite burden, while neither free CpG nor empty NP showed therapeutic effects. NP-encapsulation led to CpG persistence at the site of infection along with an unexpected preferential cellular uptake by myeloid derived suppressor cells (MDSCs; $CD11b^{+}Ly6G^{+}Ly6C^{-}$) as well as $CD19^{+}$ dendritic cells. This corresponded with the suppression of the ongoing immune response measured by the reduction of pathogenic cytokines IL-10 and IL-13, as well as IL-17 and IFNγ, in comparison to other treatment groups. As chronic inflammation is generally associated with the accumulation of MDSCs, this study may enable the rational design of cost-effective, safe, and scalable delivery systems for the treatment of inflammation-mediated diseases.

Corresponding Author: Dr. Diane McMahon-Pratt, Yale School of Public Health, Department of Epidemiology of Microbial Diseases-LEPH 811, 60 College Street, New Haven, CT, USA 06520-8034, Tel: (203) 785-4481, diane.mcmahon-pratt@yale.edu.
[5]Equally contributed to this work.

Keywords

nanoparticles; leishmaniasis; immunotherapy; CpG; PAMP; parasite

Introduction

An estimated 310 million people are at risk for leishmaniasis [1], an infection caused by obligate intracellular protozoan parasites of the *Leishmania* genus. Transmitted to mammals by sandfly bite, flagellated *Leishmania* promastigotes are phagocytosed by macrophages and neutrophils, after which the organisms transform into amastigotes and replicate. Parasites have evolved to manipulate and evade the host immune response, leading to established infection and consequent pathology [2].

In Central and South America, infection with parasites of the *Leishmania (Viannia)* complex (*L. V. panamensis*, *L. V. braziliensis*, *L. V. guyanensis*) cause cutaneous and mucocutaneous lesions. Current treatments for leishmaniasis, including antimonial drugs such as meglumine antimoniate (Glucantime®) and sodium stibogluconate (Pentostam®), are inadequate because of high systemic toxicity, expense, and requirements of parenteral administration [3]. Miltefosine (hexadecylphosphocholine; Impavido®) is the only approved oral drug, and despite leishmanicidal activity, teratocarcinogenic adverse effects impede its widespread use. Complicating treatment, resistance to many of these drugs has been reported [4, 5].

Infection with *L. (Viannia)* organisms results in hyper-inflammatory responses [6, 7], and ancillary treatments have been directed towards controlling the associated inflammation in combination with leishmanicidal drugs. Preliminary clinical studies in patients infected with *L. (Viannia)* organisms have indicated that the use of pentoxifylline, known to inhibit TNF-α (as well as IFNγ and other cytokines), together with additional drug treatment, can facilitate healing [8, 9]. Alternate approaches have leveraged the innate immune system and pathogen associated molecular patterns (PAMPs), such as the Toll-Like Receptor 9 (TLR9) agonist CpG, to facilitate the resolution of established *Leishmania* (*L. major*, *L. donovani*) infection [10–12].

More recently, *Leishmania* treatment strategies have focused on new drug delivery systems along with immune modulation to reduce toxicity and enhance treatment efficacy [13]. Delivery systems that localize and/or amplify the effects of immunomodulators have great potential for the treatment of leishmaniasis. Nanoparticles (NPs), usually solid polymeric or liposomal spheres, have been extensively demonstrated as effective in drug delivery and vaccine applications [14], and these particles possess uniquely beneficial features for anti-parasitic therapy [15, 16]. Phagocytic cells, including macrophages and dendritic cells (DCs), express TLRs and efficiently endo-, phago-, and pinocytose NPs in the size range of 50–500 nanometers (nm), enabling high intracellular concentrations of NP encapsulants that are protected from degradation and shielded to limit non-specific immune activation [17]. Additionally, NPs may enhance the efficacy of encapsulated drug through two potential mechanisms; first, prolonged polymer degradation enables sustained release and persistence of encapsulated therapeutics, and second, NPs create increased localized drug concentration. Previous work [18, 19] showed that as drug-loaded NPs enter ligand-receptor interaction

distances or penetrate a cell, the local drug concentration is significantly elevated, up to 1000-fold compared to the same concentration of free drug. As such, either mechanism (or both) may improve efficacy of a small concentration of CpG [20, 21]. NPs have been explored in *Leishmania* models, including chitosan NP for delivery of the drug amphotericin B (AmpB) [22], as vaccine systems [23, 24], and treatment of visceral disease with liposomes [25].

Given the efficacy of soluble CpG treatment in leishmaniasis models, we hypothesized that poly(lactic-co-glycolic) acid (PLGA) NPs loaded with CpG (NP-CpG) could promote healing in the *L. (V.) panamensis* chronic infection mouse model. We report that CpG encapsulated into PLGA altered Antigen-Presenting Cell (APC) targeting of CpG and increased CpG retention at lesion sites. NP-CpG effectively suppressed the development/growth of established lesions and reduced parasite burdens in treated mice. Successful treatment was accompanied by enhanced CpG uptake and expansion of $CD19^+$ dendritic and myeloid-derived suppressor cell (MDSC)-like cells, leading to a reduction in cytokine responses. Notably, MDSCs accumulate in other chronic inflammatory diseases (such as arthritis, diabetes, and multiple sclerosis), but may be sub-optimally active [26], making them potential targets for treatment [27]. Interestingly, treatment of *L. panamensis* infected mice with NP-CpG did not lead to preferential development of a T helper type 1 (Th1)-like response. Instead, the observed comprehensive reduction in cytokines is consistent with the demonstrated ability of CpG to control inflammatory responses in a dose-dependent manner [28–31], as well as the ameliorative down-regulation of inflammation by regulatory T cells during *L. (V.) panamensis* infection [32]. Collectively, these studies demonstrate the utility of PLGA NPs as a local delivery platform for *L. (V.) panamensis* immunotherapy and may prove useful for the treatment of other inflammation-mediated diseases.

Results

Nanoparticle fabrication and characterization

Solid, polymeric NP were formulated and loaded with CpG (1.2 – 1.45 μg/mg NP). Scanning electron microscopy images confirmed that NPs were spherical and monodisperse, with an average hydrodynamic diameter of 265 nm and negative surface charge (−18.0 mV zeta potential in water; Figure 1A). NP released CpG in a sustained manner depending on pH; after 18 days, ~15% of CpG was released at a physiologic pH of 7.4. In contrast, 41% of encapsulated CpG was released at endosomal pH 5 (Figure 1B). PLGA NPs are phagocytosed and transported to the endosomal and lysosomal cellular compartments [33, 34]. Although the precise mechanisms of acid and alkaline-induced polyester hydrolysis depend on numerous factors related to particles and environment [35], it is likely that exposure to acidic conditions accelerates polymer erosion, exposing carboxylic acid groups to create pockets of high acidity [36, 37]. This increased acidity not only accelerates further hydrolysis of polymer, but also protonates polymer and CpG, ultimately creating repulsive interactions to expel CpG [20]. Although extracellular release of CpG would occur with the CpG-NP formulations, the pH profile suggests that maximal release of CpG would occur upon intracellular uptake by phagocytes.

NP-CpG controls disease

The therapeutic efficacy of NP-CpG was evaluated in the *L. (V.) panamensis* mouse model. Initial studies indicated that treatment of *L. (V.) panamensis*-infected mice (at the time of infection or following lesion establishment) with CpG could ameliorate disease (Supplemental Figure 1), consistent with studies of other *Leishmania* species ([11, 12, 38–40]). In the present study, following lesion development (4–5 weeks post-infection), mice were injected perilesionally 4 times over a period of 2 weeks with either PBS (control), empty NP, NP-CpG, or soluble CpG dose-matched with NP-CpG (93 ng). The dose of CpG was based on limitations in injection volume (10 μL) and the level of CpG encapsulation within the PLGA NPs. However, given the established synergistic effects of NP incorporation [20, 21] with immunomodulatory compounds, it was of interest to determine whether this low dose of CpG might lead to disease amelioration compared to treatment with soluble CpG.

Mice treated with NP-CpG exhibited significantly reduced lesion sizes compared to control mice (Figure 2A); neither the equivalent concentration of free CpG nor empty NP alone was effective at disease remediation. Further, NP-CpG significantly reduced parasite burden in comparison to PBS, free CpG or NP alone (Figure 2B). Thus, both the particle and CpG appeared to be required for healing of established lesions.

NP- CpG modulates cytokine profiles in draining lymph nodes (dLN)

As the immune response impacts pathogenesis/healing of leishmaniasis, we next investigated how NP encapsulation affected CpG-induced cytokine profiles. In initial *in vitro* experiments, NP alone did not contribute to the immunomodulation of the antigen-specific response by CpG (Supplemental Figure 2). Consequently, experiments focused on effects *in vivo* as a result of treatment with either NP-CpG, free-CpG or NP alone.

Chronically-infected BALB/c mice were injected perilesionally with NP-CpG (containing 93 ng CpG), 93 ng free CpG, empty NP, or PBS control, and the recall cytokine responses of draining lymph nodes (dLN) cells were examined at 2 days post-treatment. Cells from mice treated with either free CpG or PBS control (Figure 3A) showed comparable levels of IFNγ; in contrast, the level of IFNγ was significantly reduced in mice treated with NP-CpG. Similarly, there was a trend toward reduced IL-17 production in CpG-NP treated mice (Figure 3B). Treatment with free CpG or NP-CpG led to significant downregulation of the anti-inflammatory cytokine IL-10 (approximately 2-fold in comparison to the PBS control; Figure 3C). Critically, NP-CpG, but not free CpG nor empty NP, significantly lowered IL-13 production (Figure 3D). In previous studies, it has been shown that both IL-10 and IL-13 are important in the development of chronic infection caused by *L. (V.) panamensis* [6], as well as infection with other *Leishmania* species [41]. Hence the reduction of these cytokines by NP-CpG treatment is likely important for NP-CpG-mediated control of disease.

It should be noted, however, that in a previous study, a reduction in IFNγ, IL-17, IL-10, and IL-13 that correlated with a significant reduction parasite burden for *L. (V.) panamensis* were observed in response to increasing regulatory T cells using IL-2 complex treatment [32]; these results suggest that lowering both inflammatory and anti-inflammatory cytokines

can lead to disease resolution in the *L. (V.) panamensis* model. Further, a hyper-inflammatory response has been shown to be important in the establishment of infection and development of disease in leishmaniasis [42], particularly in the case of the *Leishmania (Viannia)* subgenus [43]. The fact that NP-CpG is generally more effective in decreasing these cytokines than either NP alone or low dose CpG suggests that NP encapsulation of CpG enhances its potency, either by synergistic effects with polymer and degradation products, and/or persistent dosage of CpG and changes in cellular biodistribution. To further investigate these possibilities, we examined the localization of free versus NP-encapsulated CpG *in vivo*.

These results differ from previous studies employing CpG delivered in liposomes [25], where a Th1 response was induced; however, multiple differences between this previous work, including the delivery system of dipalmitoylphosphatidylcholine and cholesterol, route of delivery (intraperitoneal versus cutaneous), and level of CpG (10 μg versus 93 ng) administered could account for the differential impact on the immune response.

NP-incorporated CpG is retained in the vicinity of parasite lesions

To determine if the differences in immune responses between free CpG and NP-CpG treated mice were due to altered biodistribution, we formulated NPs with CpG conjugated to Alexa Fluor 647 (CpG-AF647) and examined the timecourse of CpG persistence at the lesion site. Mice with established lesions were injected perilesionally with dose-matched CpG-AF647 in NP or soluble form and live-imaged until fluorescence was no longer detected (Figure 4). Mice were scanned immediately before (Figures 4A, D) and directly after injection (Figures 4B, E) and monitored over 10 days. As the fluorescence intensity for commensurate doses of CpG was greater in soluble groups due to quenching from encapsulation in NPs (Supplemental Figure 3A), footpad clearance was calculated as a percentage of the initially detected fluorescence. Three days after injection, significant differences in CpG clearance between soluble and encapsulated groups were observed (Figure 4G). Imaging data showed the persistence of perilesional CpG for the NP-CpG group for at least 10 days post-injection, at which time no detectable CpG was noted in the group receiving free CpG (Figure 4G).

Ten days post-injection, animals were sacrificed and organs were scanned; commensurate levels of dosed CpG were recovered for both treatment groups (Supplemental Figures 3B and 3C). It is notable that the overall organ distribution of CpG did not significantly differ between the 2 groups within the various tissues examined (including spleen, liver, and lungs), with the exception of the lesion site. In mice dosed with soluble CpG, when signal was no longer detected at the injection site by live imaging, most recovered fluorescence was located in the dLN (but not significantly greater than NP-treated mice), whereas NP-treated mice displayed significantly more CpG retained in the feet (Supplemental Figure 3B). Overall, these results indicate that NP encapsulation of CpG creates a depot that may enable prolonged TLR9 signaling at the site of infection. These results are consistent with the established propensity of NPs to provide a depot for sustained release of encapsulants, a strategy that has been exploited for both drug and vaccine delivery systems [44] and could provide an underlying mechanism for the observed immunomodulatory efficacy.

Encapsulating CpG in NP alters cellular biodistribution

To further evaluate the biodistribution of free versus NP-encapsulated CpG, cells internalizing CpG with the 2 delivery approaches were investigated. Free CpG-AF647 or NP-encapsulated CpG-AF647 was injected perilesionally to mice at 4 weeks post-infection. Mice were sacrificed 72 hours later, the time point at which significant clearance differences were first observed between free CpG and NP-CpG (Figure 4G). Lesion and dLN cells were analyzed by flow cytometry (Figure 5) to determine the total cell populations present and the degree of CpG uptake. Phenotypic markers were used to identify TLR9-expressing cells, including B cells, polymorphonuclear leukocytes (PMN), macrophages, DCs, and myeloid-derived suppressor cells (MDSCs) (broadly defined as $CD11b^{+}Gr1^{+}$ immune regulatory cells [45, 46]). As the definition of MDSCs is somewhat controversial, for the purposes of this study, we will refer to monocytic $CD11b^{+}Ly6C^{+}Ly6G^{-}$ cells as Mo-MDSC-like and granulocytic $CD11c^{-}CD11b^{+}Ly6G^{+}Ly6C^{-}$ cells as gMDSC-like cells.

Because mice had established infections before treatment with either free CpG or NP-CpG, commensurate cell populations were expected between groups. Indeed, when gating on cells positive for CD11c, no differences were found in the portion of DCs ($CD11c^{+}CD19^{-}$ cells) present within the lesions (Figure 5A) for either treatment group. In contrast, the distribution of cell subpopulations differed for the $CD11b^{+}$ (macrophage, granulocytic) cells. NP-CpG-treated mice displayed a higher proportion of certain populations of $CD11c^{-}CD11b^{+}$ cells, including those positive for Ly6G, which have been classified as neutrophils/granulocytes and gMDSC [46] (Figure 5A).

Further analysis of the lesion cells that were positive for CpG yielded interesting results. Consistent with the significant increases in granulocytic cell populations, a higher proportion of CpG positive $CD11b^{+}$ cells were $Ly6G^{+}$ in NP-CpG treated mice, indicating that NP-CpG treatment likely expands and/or recruits $Ly6G^{+}$ granulocytic cell populations and that these cells phagocytose the NP (Figures 5A and 5B). In comparison, the greatest amount of soluble CpG was detected within the expanded populations of $CD11b^{+}Ly6G^{-}$ cells, which include Mo-MDSC-like or activated monocytes/macrophages (Figure 5B). CpG uptake in classic $CD11c^{+}$ DCs and classic macrophages ($CD11c^{-}CD11b^{+}Ly6G^{-}Ly6C^{-}$) were comparable for both groups of mice. Although there was a trend for a higher proportional level of CpG uptake in $CD19^{+}$ DCs at the site of infection in the NP-CpG group in comparison to mice receiving free CpG, this was not statistically significant.

In contrast to treatment-induced variations in cell populations within lesions, no significant differences in dLN cell populations were observed between treatment groups (Figure 5C). However, there were significant differences in CpG accumulation in dLN cell populations. NP-CpG preferentially entered granulocytic subpopulations ($Ly6G^{+}Ly6C^{+}$ and $Ly6G^{+}Ly6C^{-}$; Figure 5D) as well as a subset of plasmacytoid DCs that were $CD11c^{+}CD19^{+}$ [28, 47] (Figure 5D). The ratio of CpG-containing $CD19^{+}CD11c^{+}$/CD19-$CD11c^{+}$ cells was 2.6 for the NP-CpG treatment group compared to a ratio of 1.1 for free CpG-treated mice (Figure 5D).

Collectively, there was enhanced delivery of NP-CpG to both $CD19^{+}$ DCs and MSDC-like cells at both the lesion site and dLN. High doses of free CpG have been reported to increase

IDO expression in $CD19^+$ DCs, leading to the induction of suppressive immune responses [48, 49]. Additionally, gMDSCs can suppress ongoing immune responses. MDSCs have also been shown to be involved in the induction of T regulatory cells [50]; however, we failed to find an increase in T regulatory levels in the dLN of the NP-CpG treated mice in comparison to controls (Supplemental Figure 4). As treatment with NP-CpG leads to the suppression of IFNγ, IL-10, and IL-13 (Figure 3), it is likely that NP-CpG targeting and expansion of suppressive $CD19^+$ DCs and MDSC-like cells contribute to the modulation of the immune response.

Discussion

Rationally engineered NPs provide a promising vaccine and immunotherapy strategy [23] that can be applied to parasitic infections. As soluble CpG treatment has been shown to ameliorate established disease in the case of *L. major* [11], *L. donovani* [12], and *L. (V.) panamensis* [40], we formulated CpG-loaded NPs to provide long-term immunomodulatory therapy. Limited by CpG loading restrictions and injection volume, a maximum of 93 ng of CpG (encapsulated in NP) could be delivered intralesionally per mouse. This dose is approximately 100 to 500-fold less than that which is historically used for CpG immunotherapy and, unsurprisingly, this 93 ng dose of soluble CpG alone did not exhibit therapeutic efficacy. However, encapsulation into PLGA NPs bestowed 93 ng of CpG with therapeutic efficacy in *L. (V.) panamensis*-infected BALB/c mice. Overall, NP-CpG treatment resulted in downregulation of IL-10 and IL-13, which previous immunogenic studies have revealed to be key promoters of *L. (V.) panamensis* infection [6]. Additionally, reductions in the IFNγ (and to a lesser extent, IL-17) response were observed in this group, suggesting a general suppression or downregulation of the ongoing immune response. This aligns with recent studies in patients [51] and in the mouse model [32] demonstrating that an overall anti-inflammatory response can be associated with healing. Additionally, the chronicity of *L. (V.) panamensis* infection has been associated with induction of chemokines [52], IFNγ is known to lead to increases in vascular permeability, chemokine levels, and cellular infiltration [53–55] associated with inflammation. Consequently, the reduction of these cytokines and the ongoing immune response by NP-CpG treatment is likely important for the disease control observed.

The ability of NP-CpG to more effectively decrease these cytokines than either NP alone or free CpG suggests that NP encapsulation enhances the potency of CpG through persistent dosage of CpG and/or changes in cellular biodistribution. Indeed, when encapsulated in NPs, more CpG remained at the site of infection after injection. The sustained release of CpG by NP hydrolysis enabled continuous delivery of CpG, potentially optimizing TLR9 engagement to contribute to the enhanced efficacy observed.

Further, the CpG delivery platform employed (saline versus NP) led to changes in cell populations present in the lesion site as well as in the cellular distribution of CpG. Notably, in the NP-CpG group, the distribution within the $CD11b^+$ population (macrophages and granulocytes) was associated with an increased proportion of $Ly6G^+$ cells, which includes neutrophils/granulocytes and granulocytic MDSCs [46]. The increase in MDSC-like cells is consistent with studies indicating that activation via CpG [56] and/or through NLRP3 [57]

can drive the expansion of MDSCs [58–60] via the induction of IL-1β. Interestingly, IL-1β has been shown to have variable roles in leishmaniasis, dependent upon the infective species [61–63]; notably, IL-1β was found to ameliorate *L. (V.) braziliensis* infection [63] but have an opposing effect for *L. major*, where MDSCs have been shown to exacerbate disease [62]. Further, the roles of PMNs in cutaneous leishmaniasis also appear to be variable and dependent on infecting species [61, 64, 65]; PMNs have been shown to enhance *L. major* infection and suppress *L. (V.) braziliensis* infection. It should be noted, however, that in these studies MDSCs and PMNs were not distinguished.

Consistent with the significant increases in total granulocytic cell populations, a higher proportion of CpG-positive cells were $CD11b^+Ly6G^+$ in mice treated with NP-CpG. Although the response of MDSCs to NLRP3 and TLR9 stimulation is complex [58], the decrease in cytokine responses observed here is consistent with enhanced MDSC activity. Interestingly, the distribution of CpG within lesion macrophages was comparable for both the free CpG and NP-CpG treatment groups; therefore, the therapeutic differences found do not appear to involve direct targeting and modulation of the primary host cell of the parasite.

In contrast to findings in the dLN, no differences in the distribution of various cell populations were found at the lesion site between the mice receiving free CpG or NP-CpG. However, there remained a similar pattern of platform-selected targeting for the $CD11b^+$ $Ly6G^+$ cell populations in the NP-CpG group. Further, NP-CpG preferentially entered a subset of plasmacytoid DCs (pDCs), which were $CD11c^+CD19^+$ [28, 47]. While soluble CpG was also found in this subpopulation of DCs, the ratio of CpG^+ cells ($CD19^+CD11c^+$ to CD19-$CD11c^+$) was approximately 2.5 times greater for the NP-CpG treatment group than the free CpG treatment group, indicating selective targeting and uptake of NP-CpG. The role of DCs in the regulation of leishmaniasis is complex, and is determined in part by the DC population [66–68]. CpG has been reported to increase IDO expression in $CD19^+$ pDCs, leading to the induction of T regulatory cells and suppressive immune responses [48, 49], which partially act through the induction of type I interferons. While these studies involved high doses of free CpG, given the increased CpG uptake by these cells due to NP encapsulation and their known role in suppression, tolerogenic pDCs are of mechanistic interest. The overall ameliorative effects of NP-CpG on both pDCs and MDSCs is likely impacted by concurrent NLRP3 activation and the pre-existing inflammatory microenviroment caused by established *L. (V.) panamensis* infection.

Conclusion

This work demonstrated the efficacy of CpG-loaded PLGA NPs to ameliorate established *Leishmania (V.) panamensis* infection. The sustained release of CpG created a beneficial kinetic profile of receptor engagement at tissue, cellular, and intracellular levels, with preferential targeting of MDSCs and plasmacytoid DCs, corresponding to the down-regulation of the inflammatory response. NP encapsulation bestowed a sub-therapeutic dose of CpG, 93 ng, with observable efficacy. Future generations of therapeutic NP could contain CpG combined with other adjuvants and anti-leishmanial drugs to lower chemotherapeutic doses, increase parasite killing, and reduce toxicity. Critically, NP-CpG was therapeutic as a local rather than systemic treatment, which could further limit adverse effects. As MDSCs

have been shown to accumulate during other chronic inflammation, NP-CpG may have utility as a safe and effective treatment strategy for a variety of immune-mediated diseases.

Materials and Methods

Materials

Fully phosphorothioated 3′ Type B CpG 1826 ODN was purchased from Invivogen (sequence: 5′ TCC ATG ACG TTC CTG ACG TT 3′). Poly(vinyl alcohol) (PVA) and chloroform were purchased from Sigma-Aldrich (St. Louis, MO). Research-grade PLGA (50:50, iv .55–.75 dL/g) was purchased from Durect (Pelham, AL). The following fluorochrome-conjugated antibodies were employed: CD11c-PE-Cy7 (BD Biosciences; clone HL3), Ly6C-PerCP-Cyanine5.5 (eBioscience; clone HK1.4), Ly6G-PE (BioLegend; clone 1A8), CD11b-eFluor450 (eBioscience; clone M1/70), CD19-FITC (eBioscience; clone 1D3).

Nanoparticle Fabrication and Characterization

PLGA NPs were synthesized using a water/oil/water (w/o/w) double emulsion technique previously described [57]. The CpG utilized was CpG 1826, a type B CpG with a phosphorylthiolate backbone, which has been shown to have superior stability [69] and documented ability to stimulate macrophages and dendritic cells in addition to B cells [70, 71]. Briefly, polymer was dissolved in chloroform at 50 mg/mL. CpG 1826 (8 mg/mL in PBS) or PBS was added dropwise to the polymer solution under vortex, followed by 30 seconds of sonication using a Tekmar Sonic Distributor fitted with a CV26 sonicator at 38% amplitude. The dissolved polymer/encapsulant was added dropwise to an aqueous 5% PVA solution under vortex before a second round of sonication. Residual chloroform evaporated as NPs hardened in 0.2% stirring PVA in a fume hood. NP were collected and rinsed by centrifugation at 12,000 rpm for 20 minutes, flash frozen, lyophilized in pre-weighed vials, and stored at −20°C. NPs were characterized by Scanning Electron Microscopy and with a Malvern Zetasizer, which measures hydrodynamic diameter by dynamic light scattering and zeta potential by Laser Doppler Micro-Electrophoresis. To determine CpG loading, NP were dissolved with a mixture of 0.1N NaOH and 1% Triton-X and oligonucleotide content quantified by PicoGreen DNA Detection Assay. Blank NPs were used as negative controls. Similarly, for controlled release experiments, NP-CpG or blank NPs were suspended in PBS at pH 7.4 or pH 5 at 2 mg/mL and tumbled in a 37°C incubator. At each timepoint, NP suspensions were pelleted at 13,200 rpm, supernatant collected and frozen for future CpG quantification by PicoGreen, and then particles were resuspended in pH 5 or pH 7.4 PBS buffer and replaced into the incubator. Percent release was calculated by dividing the quantified CpG in supernatant timepoints by total CpG loading in NP.

Animals

Female BALB/c mice were obtained from the National Cancer Institute (Frederick, MD, USA) and housed at the Yale University School of Medicine facilities, approved by the American Association for Accreditation of Laboratory Animal Care. All animal procedures were performed in compliance with the U.S. Department of Health and Human Services

Guide for the Care and Use of Laboratory Animals and were reviewed and approved by the Yale University Committee for the Use and Care of Animals.

Parasite culture, infection, and parasite burden analyses

L. (V.) panamensis (strain MHOM/CO/1995/1989) were grown in Schneider's Drosophila medium supplemented with 20% heat-inactivated FCS and 17.5 μg/ml gentamycin. The infection protocol has been described previously [6]. Briefly, infective parasites were isolated from late stationary phase promastigotes from the 45/60% Percoll gradient interface. Parasites (5×10^4) were injected intradermally into the top of a hind foot. Lesion development was monitored by measuring the foot thickness using a dial gauge caliper (Starrett Thickness Gauge) and calculating the ratio between the infected and the contralateral non-infected foot. At the termination of the experiment, parasites were quantified in infected tissue by limiting dilution. Draining lymph node cells were isolated and stimulated with soluble *Leishmania* antigen (SLA), and cytokines analyzed by ELISA as previously described [6, 32].

NP-CpG Treatment

Following lesion development (between 3–5 weeks post-infection) mice were treated twice per week for 2 weeks with NP-CpG (93 ng CpG in 64 μg NP), free CpG (93 ng), empty NP (64 μg), or PBS. Due to limitations in injection volume and NP concentration (64 μg in 10 μL), a dose of 93 ng of CpG was the maximum allowed dose for perilesional injections. Two days following the final treatment, a subset of mice in each group (3–4) were sacrificed, and cells were harvested from draining lymph nodes (dLN) and stimulated with soluble *Leishmania* antigen (SLA; equivalent to 2.5×10^6 parasites/ml) for 3 days. Cytokines were measured in the culture supernatant by ELISA (Ready Set Go kits, eBioscience). In the remaining mice (5–6 mice/group), lesion size was measured weekly for 3 weeks following the end of treatment, and parasite burden was determined at the time of sacrifice, as described above.

CpG Biodistribution

To determine CpG distribution *in vivo*, NP were formulated as previously described encapsulating CpG conjugated to Alexa Fluor 647 (CpG-AF647, TriLink Biotechnologies). After lesions were established, mice were injected perilesionally with therapeutic doses of reagents (93 ng CpG-AF647 in soluble or NP form) in 10 μL. Live imaging experiments were performed using a Bruker In-Vivo MS FX Pro small animal optical imaging system, in which animals were anesthetized with vaporized isofluorane. When signal diminished from footpads 10 days post-injection, mice were sacrificed and organs harvested for scans by the Bruker system. Fluorescence was quantified by percent of initial dose, as soluble and NP-CpG provided different initial signal intensities (despite commensurate CpG concentration).

CpG-cellular distribution experiments were performed by flow cytometry. Mice with established lesions were perilesionally injected with fluorescently labeled CpG, free or NP encapsulated, and euthanized 3 days later. Draining lymph node cells were isolated by mechanical disruption of dLN through a cell strainer, followed by ACK lysis. Cells were stained by incubating with a solution of fluorescently-tagged antibodies (CD11c-PE-Cy7,

Ly6C-PE-Cy5.5, Ly6G-PE, CD11b-eFluor450, CD19-FITC), and samples run on LSR II Flow Cytometer. Data was analyzed using FlowJo Software (Tree Star, Inc.), and gating strategies are outlined in Supplemental Figure 5.

Statistical Analyses

Statistical analyses were conducted using the Students t-test. For parasite burden analysis, data was log transformed prior to the t-test. P values ≤0.05 were considered significant.

Supplementary Material

Refer to Web version on PubMed Central for supplementary material.

Acknowledgments

The authors would like to thank Dr. Nancy Ruddle and Sean Bickerton for critical review of our paper and useful discussions. This work was supported by the National Institute of Allergy and Infectious Diseases (R01AI093775). AE was supported in part through T32 AI07404 training grant.

References

1. WHO Leishmaniasis. World Health Organization; 2016. Leishmaniasis. http://www.who.int/leishmaniasis/surveillance/en/
2. Kaye P, Scott P. Leishmaniasis: complexity at the host-pathogen interface. Nat Rev Microbiol. 2011; 9:604–15. [PubMed: 21747391]
3. Sundar S, Chakravarty J. Leishmaniasis: an update of current pharmacotherapy. Expert Ppin Pharmacother. 2013; 14:53–63.
4. Sundar S, Singh A, Singh OP. Strategies to overcome antileishmanial drugs unresponsiveness. J Trop Med. 2014; 2014:646932.doi: 10.1155/2014/646932 [PubMed: 24876851]
5. Walker J, Gongora R, Vasquez JJ, Drummelsmith J, Burchmore R, Roy G, et al. Discovery of factors linked to antimony resistance in *Leishmania panamensis* through differential proteome analysis. Mol Biochem Parasitol. 2012; 183:166–76. [PubMed: 22449941]
6. Castilho TM, Goldsmith-Pestana K, Lozano C, Valderrama L, Saravia NG, McMahon-Pratt D. Murine model of chronic *L. (Viannia) panamensis* infection: role of IL-13 in disease. Eur J Immunol. 2010; 40:2816–29. [PubMed: 20827674]
7. Bosque F, Saravia NG, Valderrama L, Milon G. Distinct innate and acquired immune responses to Leishmania in putative susceptible and resistant human populations endemically exposed to L. (Viannia) panamensis infection. Scand J Immunol. 2000; 51:533–41. [PubMed: 10792848]
8. Lessa HA, Machado P, Lima F, Cruz AA, Bacellar O, Guerreiro J, et al. Successful treatment of refractory mucosal leishmaniasis with pentoxifylline plus antimony. Amer J Trop Med Hyg. 2001; 65:87–9. [PubMed: 11508396]
9. Brito G, Dourado M, Polari L, Celestino D, Carvalho LP, Queiroz A, et al. Clinical and immunological outcome in cutaneous leishmaniasis patients treated with pentoxifylline. Amer J Trop Med Hyg. 2014; 90:617–20. [PubMed: 24567316]
10. Flynn B, Wang V, Sacks DL, Seder RA, Verthelyi D. Prevention and treatment of cutaneous leishmaniasis in primates by using synthetic type D/A oligodeoxynucleotides expressing CpG motifs. Infect Immun. 2005; 73:4948–54. [PubMed: 16041009]
11. Zimmermann S, Egeter O, Hausmann S, Lipford GB, Rocken M, Wagner H, Heeg K. Cutting Edge: CpG oligodeoxynucleotides trigger protective and curative Th1 responses in lethal murine leishmaniasis. J Immunol. 1998; 160:3627–30. [PubMed: 9558060]
12. Datta N, Mukherjee S, Das L, Das PK. Targeting of immunostimulatory DNA cures experimental visceral leishmaniasis through nitric oxide up-regulation and T cell activation. Eur J Immunol. 2003; 33:1508–1518. [PubMed: 12778468]

13. Moreno E, Schwartz J, Fernandez C, Sanmartin C, Nguewa P, Irache JM, et al. Nanoparticles as multifunctional devices for the topical treatment of cutaneous leishmaniasis. Expert Opin Drug Deliv. 2014; 11:579–597. [PubMed: 24620861]
14. Siefert AL, Caplan MJ, Fahmy TM. Artificial bacterial biomimetic nanoparticles synergize Pathogen-Associated Molecular Patterns for vaccine efficacy. Biomaterials. 2016; 97:85–96. [PubMed: 27162077]
15. Date AA, Joshi MD, Patravale VB. Parasitic diseases: Liposomes and polymeric nanoparticles versus lipid nanoparticles. Adv Drug Deliv Rev. 2007; 59:505–521. [PubMed: 17574295]
16. Zazo H, Colino CL, Lanao JM. Current applications of nanoparticles in infectious diseases. J Controlled Release. 2016; 224:86–102.
17. Elamanchili P, Diwan M, Cao M, Samuel J. Characterization of poly(D,L-lactic-co-glycolic acid) based nanoparticulate system for enhanced delivery of antigens to dendritic cells. Vaccine. 2004; 22:2406–2412. [PubMed: 15193402]
18. Labowsky M, Lowenthal J, Fahmy TM. An in silico analysis of nanoparticle/cell diffusive transfer: application to nano-artificial antigen-presenting cell:T-cell interaction. Nanomedicine. 2015; 11:1019–28. [PubMed: 25652896]
19. Steenblock ER, Fadel T, Labowsky M, Pober JS, Fahmy TM. An artificial antigen-presenting cell with paracrine delivery of IL-2 impacts the magnitude and direction of the T cell response. J Biol Chem. 2011; 286:34883–34892. [PubMed: 21849500]
20. de Titta A, Ballester M, Julier Z, Nembrini C, Jeanbart L, van der Vlies AJ, et al. Nanoparticle conjugation of CpG enhances adjuvancy for cellular immunity and memory recall at low dose. Proc Natl Acad Sci USA. 2013; 110:19902–19907. [PubMed: 24248387]
21. Gursel I, Gursel M, Ishii KJ, Klinman DM. Sterically stabilized cationic liposomes improve the uptake and immunostimulatory activity of CpG oligonucleotides. J Immunol. 2001; 167:3324–3328. [PubMed: 11544321]
22. Ribeiro TG, Chavez-Fumagalli MA, Valadares DG, Franca JR, Rodrigues LB, Duarte MC, et al. Novel targeting using nanoparticles: an approach to the development of an effective anti-leishmanial drug-delivery system. Internatl J Nanomed. 2014; 9:877–890.
23. Heravi Shargh V, Jaafari MR, Khamesipour A, Jalali SA, Firouzmand H, Abbasi A, et al. Cationic liposomes containing soluble *Leishmania* antigens (SLA) plus CpG ODNs induce protection against murine model of leishmaniasis. Parasitol Res. 2012; 111:105–114. [PubMed: 22223037]
24. Santos DM, Carneiro MW, de Moura TR, Soto M, Luz NF, Prates DB, et al. PLGA nanoparticles loaded with KMP-11 stimulate innate immunity and induce the killing of *Leishmania*. Nanomedicine. 2013; 9:985–995. [PubMed: 23603355]
25. Shivahare R, Vishwakarma P, Parmar N, Yadav PK, Haq W, Srivastava M, et al. Combination of liposomal CpG oligodeoxynucleotide 2006 and miltefosine induces strong cell-mediated immunity during experimental visceral leishmaniasis. PLoS ONE. 2014; 9:e94596. [PubMed: 24732039]
26. Whitfield-Larry F, Felton J, Buse J, Su MA. Myeloid-derived suppressor cells are increased in frequency but not maximally suppressive in peripheral blood of Type 1 Diabetes Mellitus patients. Clin Immunol. 2014; 153:156–164. [PubMed: 24769355]
27. Boros P, Ochando J, Zeher M. Myeloid derived suppressor cells and autoimmunity. Hum Immunol. 2016; 8:631–666. [PubMed: 27240453]
28. Baban B, Chandler PR, Sharma MD, Pihkala J, Koni PA, Munn DH, et al. IDO activates regulatory T cells and blocks their conversion into Th17-like T cells. J Immunol. 2009; 183:2475–2483. [PubMed: 19635913]
29. Campbell JD, Kell SA, Kozy HM, Lum JA, Sweetwood R, Chu M, et al. A limited CpG-containing oligodeoxynucleotide therapy regimen induces sustained suppression of allergic airway inflammation in mice. Thorax. 2014; 69:565–573. [PubMed: 24464743]
30. Waibler Z, Anzaghe M, Konur A, Akira S, Muller W, Kalinke U. Excessive CpG 1668 stimulation triggers IL-10 production by cDC that inhibits IFN-alpha responses by pDC. Eur J Immunol. 2008; 38:3127–3137. [PubMed: 18991289]
31. Xin L, Shelite TR, Gong B, Mendell NL, Soong L, Fang R, et al. Systemic treatment with CpG-B after sublethal rickettsial infection induces mouse death through indoleamine 2,3-dioxygenase (IDO). PloS One. 2012; 7:e34062. [PubMed: 22470514]

32. Ehrlich A, Castilho TM, Goldsmith-Pestana K, Chae W-J, Bothwell ALM, Sparwasser T, et al. The immunotherapeutic role of regulatory T cells in *Leishmania (Viannia) panamensis* infection. J Immunol. 2014; 193:2961–2970. [PubMed: 25098291]
33. Demento SL, Eisenbarth SC, Foellmer HG, Platt C, Caplan MJ, Saltzman WM, et al. Inflammasome-activating nanoparticles as modular systems for optimizing vaccine efficacy. Vaccine. 2009; 27:3013–3021. [PubMed: 19428913]
34. Cartiera MS, Johnson KM, Rajendran V, Caplan MJ, Saltzman WM. The uptake and intracellular fate of PLGA nanoparticles in epithelial cells. Biomaterials. 2009; 30:2790–2798. [PubMed: 19232712]
35. Zolnik BS, Burgess DJ. Effect of acidic pH on PLGA microsphere degradation and release. J Controlled Release. 2007; 122:338–344.
36. Li L, Schwendeman SP. Mapping neutral microclimate pH in PLGA microspheres. Journal of controlled release: official journal of the Controlled Release Society. 2005; 101:163–73. [PubMed: 15588902]
37. Holy CE, Dang SM, Davies JE, Shoichet MS. In vitro degradation of a novel poly(lactide-co-glycolide) 75/25 foam. Biomaterials. 1999; 20:1177–85. [PubMed: 10395386]
38. Wu W, Weigand L, Belkaid Y, Mendez S. Immunomodulatory effects associated with a live vaccine against Leishmania major containing CpG oligodeoxynucleotides. Eur J Immunol. 2006; 36:3238–47. [PubMed: 17109471]
39. Wu W, Huang L, Mendez S. A live Leishmania major vaccine containing CpG motifs induces the de novo generation of Th17 cells in C57BL/6 mice. Eur J Immunol. 2010; 40:2517–27. [PubMed: 20683901]
40. Ehrlich, A. Yale University. The Role of Regulatory T Cells during Leishmania (Viannia) panamensis Infection: A Target for Immunotherapy. p. 1online resource (158 p.)
41. Hurdayal R, Brombacher F. The role of IL-4 and IL-13 in cutaneous Leishmaniasis. Immunology letters. 2014; 161:179–83. [PubMed: 24412597]
42. Ribeiro-Gomes FL, Roma EH, Carneiro MB, Doria NA, Sacks DL, Peters NC. Site-dependent recruitment of inflammatory cells determines the effective dose of Leishmania major. Infection and immunity. 2014; 82:2713–27. [PubMed: 24733090]
43. Oliveira WN, Ribeiro LE, Schrieffer A, Machado P, Carvalho EM, Bacellar O. The role of inflammatory and anti-inflammatory cytokines in the pathogenesis of human tegumentary leishmaniasis. Cytokine. 2014; 66:127–32. [PubMed: 24485388]
44. Demento SL, Cui W, Criscione JM, Stern E, Tulipan J, Kaech SM, et al. Role of sustained antigen release from nanoparticle vaccines in shaping the T cell memory phenotype. Biomaterials. 2012; 33:4957–64. [PubMed: 22484047]
45. Ray A, Chakraborty K, Ray P. Immunosuppressive MDSCs induced by TLR signaling during infection and role in resolution of inflammation. Frontiers in cellular and infection microbiology. 2013; 3:52. [PubMed: 24066282]
46. Talmadge JE, Gabrilovich DI. History of myeloid-derived suppressor cells. Nature Reviews Cancer. 2013; 13:739–52.
47. Kahler DJ, Mellor AL. T cell regulatory plasmacytoid dendritic cells expressing indoleamine 2,3 dioxygenase. Handbook of experimental pharmacology. 2009:165–96. [PubMed: 19031026]
48. Baban B, Chandler PR, Johnson BA, Huang L, Li M, Sharpe ML, et al. Physiologic control of IDO competence in splenic dendritic cells. Journal of immunology. 2011; 187:2329–35.
49. Johnson BA 3rd, Kahler DJ, Baban B, Chandler PR, Kang B, Shimoda M, et al. B-lymphoid cells with attributes of dendritic cells regulate T cells via indoleamine 2,3-dioxygenase. Proceedings of the National Academy of Sciences of the United States of America. 2010; 107:10644–8. [PubMed: 20498068]
50. Yin B, Ma G, Yen C-Y, Zhou Z, Wang GX, Divino CM, et al. Myeloid-derived suppressor cells prevent type 1 diabetes in murine models. The Journal of Immunology. 2010; 185:5828–34. [PubMed: 20956337]
51. Rodriguez-Pinto D, Navas A, Blanco VM, Ramirez L, Garcerant D, Cruz A, et al. Regulatory T cells in the pathogenesis and healing of chronic human dermal leishmaniasis caused by

Leishmania (Viannia) species. PLoS neglected tropical diseases. 2012; 6:e1627. [PubMed: 22545172]

52. Navas A, Vargas DA, Freudzon M, McMahon-Pratt D, Saravia NG, Gomez MA. Chronicity of dermal leishmaniasis caused by *Leishmania panamensis* is associated with parasite-mediated induction of chemokine gene expression. Infection and immunity. 2014; 82:2872–80. [PubMed: 24752514]
53. Lazarevic V, Glimcher LH. T-bet in disease. Nature immunology. 2011; 12:597–606. [PubMed: 21685955]
54. Martin S, Maruta K, Burkart V, Gillis S, Kolb H. IL-1 and IFN-gamma increase vascular permeability. Immunology. 1988; 64:301–5. [PubMed: 3134297]
55. Shachar I, Karin N. The dual roles of inflammatory cytokines and chemokines in the regulation of autoimmune diseases and their clinical implications. Journal of leukocyte biology. 2013; 93:51–61. [PubMed: 22949334]
56. Barber GN. Cytoplasmic DNA innate immune pathways. Immunological reviews. 2011; 243:99–108. [PubMed: 21884170]
57. Demento SL, Bonafe N, Cui W, Kaech SM, Caplan MJ, Fikrig E, et al. TLR9-targeted biodegradable nanoparticles as immunization vectors protect against West Nile encephalitis. J Immunol. 2010; 185:2989–97. [PubMed: 20660705]
58. Fernandez A, Oliver L, Alvarez R, Fernandez LE, Lee KP, Mesa C. Adjuvants and myeloid-derived suppressor cells: enemies or allies in therapeutic cancer vaccination. Human vaccines & immunotherapeutics. 2014; 10:3251–60. [PubMed: 25483674]
59. Serafini P. Myeloid derived suppressor cells in physiological and pathological conditions: the good, the bad, and the ugly. Immunologic research. 2013; 57:172–84. [PubMed: 24203443]
60. Trikha P, Carson WE 3rd. Signaling pathways involved in MDSC regulation. Biochimica et biophysica acta. 2014; 1846:55–65. [PubMed: 24727385]
61. Charmoy M, Hurrell BP, Romano A, Lee SH, Ribeiro-Gomes F, Riteau N, et al. The Nlrp3 inflammasome, IL-1beta, and neutrophil recruitment are required for susceptibility to a non-healing strain of Leishmania major in C57BL/6 mice. Eur J Immunol. 2015
62. Gurung P, Karki R, Vogel P, Watanabe M, Bix M, Lamkanfi M, et al. An NLRP3 inflammasome-triggered Th2-biased adaptive immune response promotes leishmaniasis. The Journal of clinical investigation. 2015; 125:1329–38. [PubMed: 25689249]
63. Lima-Junior DS, Costa DL, Carregaro V, Cunha LD, Silva AL, Mineo TW, et al. Inflammasome-derived IL-1beta production induces nitric oxide-mediated resistance to Leishmania. Nature medicine. 2013; 19:909–15.
64. Falcao SA, Weinkopff T, Hurrell BP, Celes FS, Curvelo RP, Prates DB, et al. Exposure to Leishmania braziliensis triggers neutrophil activation and apoptosis. PLoS neglected tropical diseases. 2015; 9:e0003601. [PubMed: 25756874]
65. Novais FO, Santiago RC, Bafica A, Khouri R, Afonso L, Borges VM, et al. Neutrophils and macrophages cooperate in host resistance against Leishmania braziliensis infection. J Immunol. 2009; 183:8088–98. [PubMed: 19923470]
66. Ashok D, Acha-Orbea H. Timing is everything: dendritic cell subsets in murine Leishmania infection. Trends in parasitology. 2014; 30:499–507. [PubMed: 25190685]
67. Carvalho LP, Pearce EJ, Scott P. Functional dichotomy of dendritic cells following interaction with Leishmania braziliensis: infected cells produce high levels of TNF-alpha, whereas bystander dendritic cells are activated to promote T cell responses. J Immunol. 2008; 181:6473–80. [PubMed: 18941238]
68. Feijo D, Tiburcio R, Ampuero M, Brodskyn C, Tavares N. Dendritic Cells and Leishmania Infection: Adding Layers of Complexity to a Complex Disease. Journal of immunology research. 2016; 2016:3967436. [PubMed: 26904694]
69. Sester DP, Naik S, Beasley SJ, Hume DA, Stacey KJ. Phosphorothioate backbone modification modulates macrophage activation by CpG DNA. The Journal of Immunology. 2000; 165:4165–73. [PubMed: 11035048]

70. Iparraguirre A, Tobias JW, Hensley SE, Masek KS, Cavanagh LL, Rendl M, et al. Two distinct activation states of plasmacytoid dendritic cells induced by influenza virus and CpG 1826 oligonucleotide. Journal of leukocyte biology. 2008; 83:610–20. [PubMed: 18029397]

71. Liu Y, Luo X, Yang C, Yu S, Xu H. Three CpG oligodeoxynucleotide classes differentially enhance antigen-specific humoral and cellular immune responses in mice. Vaccine. 2011; 29:5778–84. [PubMed: 21664398]

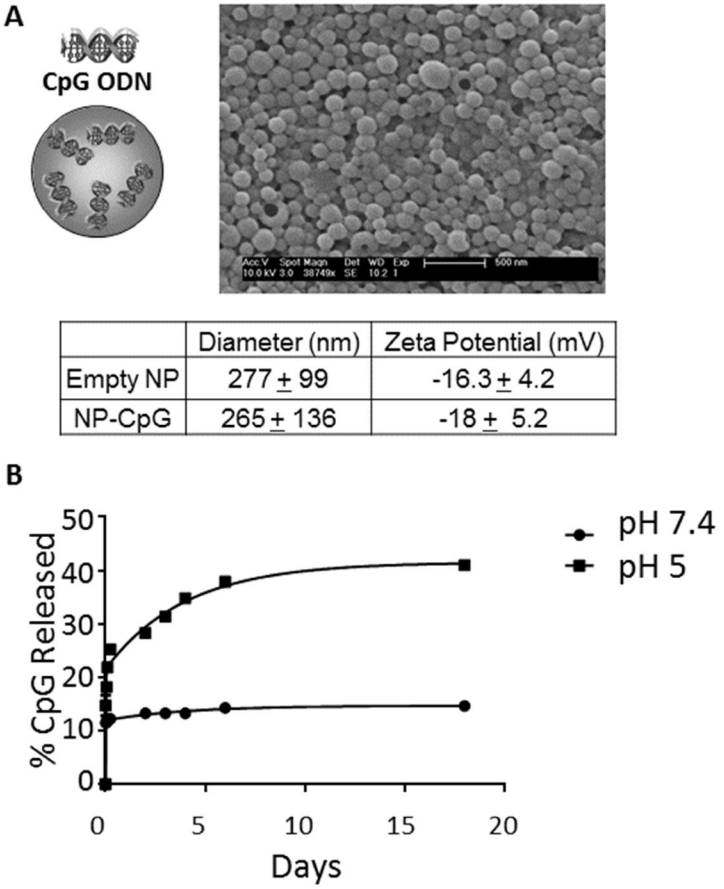

	Diameter (nm)	Zeta Potential (mV)
Empty NP	277 ± 99	-16.3 ± 4.2
NP-CpG	265 ± 136	-18 ± 5.2

Figure 1. Characteristics of NP-CpG

(A) Schematic representation PLGA NP encapsulating 1.45 μg CpG per mg NP. The size of CpG-NP was measured by scanning electron microscopy, and the charge in water was determined as described in Materials and Methods Section. Data presented are from 4 experimental replicates (averages of all particles used) and triplicate determinations per experiment. (B) CpG release from NP was measured by tumbling NP in acidic or physiologic pH at 37°C. Results are representative of 3 independent experiments. *p<.05; **p<.01; ***p<.001.

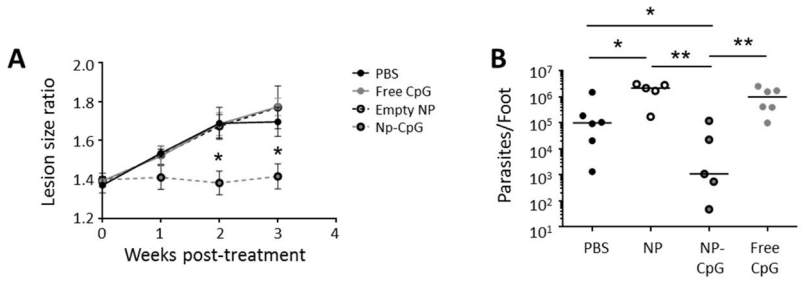

Figure 2. NP-CpG control established leishmaniasis

BALB/c mice were infected with 5×10^4 late stationary phase *L. (V.) panamensis* promastigotes. After lesions developed, mice were injected perilesionally twice a week for 2 weeks with PBS, 64 μg NP-CpG, dose-matched free CpG (93 ng), or 64 μg empty NP. (A) Lesion progression was monitored by weekly measurements of feet. (B) Three weeks post-treatment, mice were euthanized, and parasites were quantified in lesions by limiting dilution. Data are representative of 3 independent experiments. n=5–6; *p<.05; **p<.01.

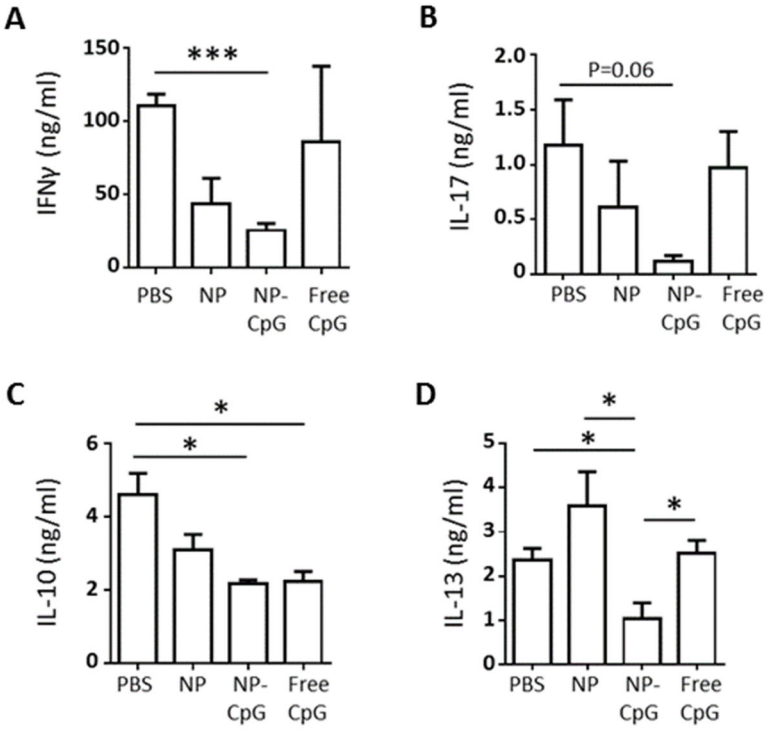

Figure 3. NP-CpG regulates cytokine responses in *L. (V.) panamensis*-infected mice

Mice with established lesions were injected perilesionally twice a week for 2 weeks with PBS, 64 μg CpG-NP, dose-matched free CpG (93 ng) or 64 μg empty NP. Two days after the end of treatment, dLN cells were harvested and stimulated with Soluble *Leishmania* Antigen (SLA) and (A) IFNγ, (B) IL-17, (C) IL-10 and (D) IL-13 levels were determined by ELISA. Data are representative of 3 independent experiments. Bars display group mean with standard error. n=3–5;*p<.05; ***p<.001.

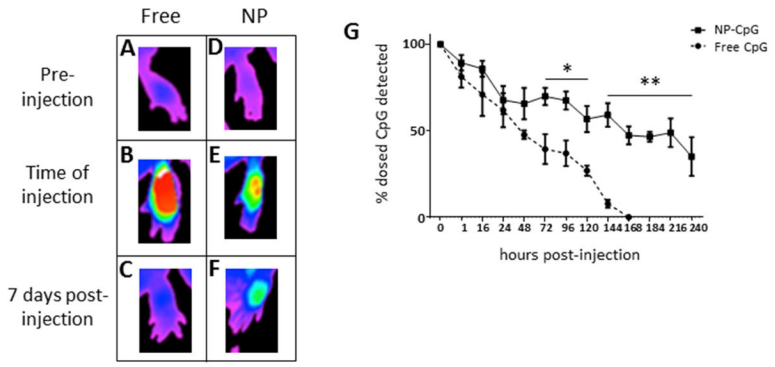

Figure 4. NP-CpG persists in the lesions of *L. (V.) panamensis*-infected mice

Fluorescently-labeled CpG, free or encapsulated in NP, was injected perilesionally into mice with established disease and animals were live imaged. (A, D) Before injection, infected mice exhibited similar background fluorescence. Immediately after injection, a greater intensity of soluble CpG was detected (C) than NP-CpG (D), owing to fluorescence quenching by NP encapsulation. Thus, clearance of fluorescence was normalized to the original detected dose for daily imaging (G), with representative images of fluorescence at day 7 (C, F). Data are representative of 3 independent experiments. n=3; *p<.05; **p<.01.

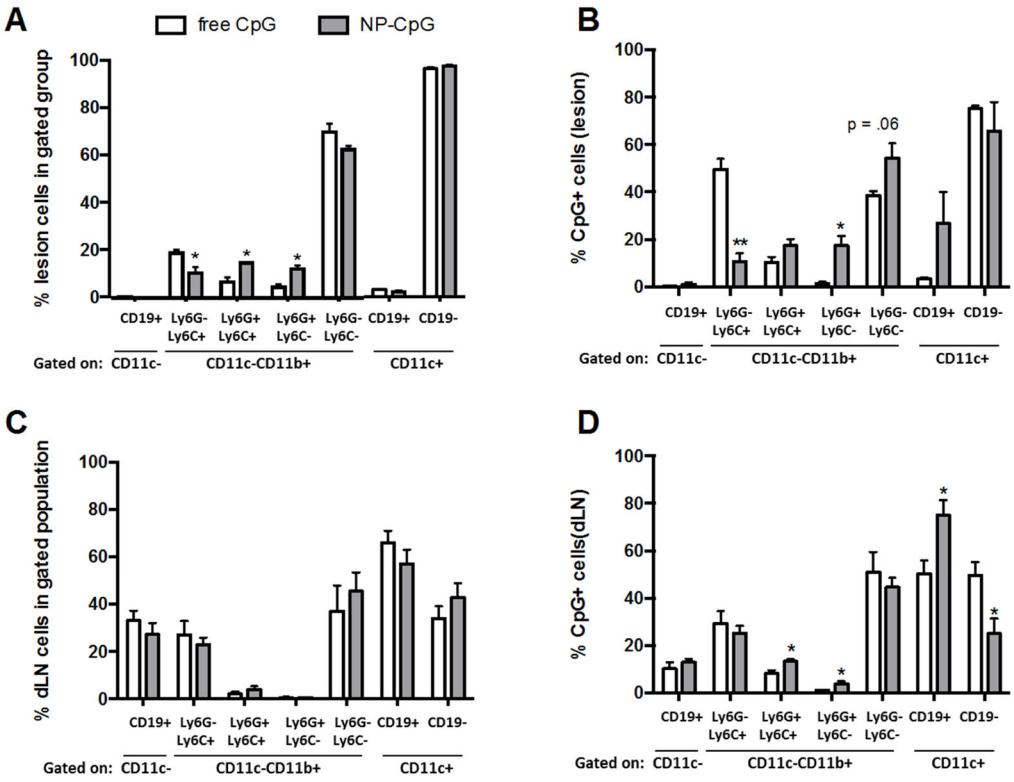

Figure 5. NP encapsulation alters the cellular distribution of CpG

The cellular distribution of labeled CpG (free or NP) was determined 72 hours following treatment of mice with established lesions. The overall distribution of cells in the foot (A) and dLN (C) of the same mice was also assessed. Cell populations in the foot (B) and dLN (D) were gated on CpG+ cells, and the cellular distribution of CpG+ cells was determined by flow cytometry, as described in Materials and Methods Section. Data are representative of 3 independent experiments. n=3; *p<.05; **p<.01.